Opt Quant Electron (2015) 47:3301–3312
DOI 10.1007/s11082-015-0208-0

Optical properties of left-handed metamaterial involving coated nano-spheres

H. Sadeghi[1] · A. Zolanvar[1] · A. Ranjgar[1]

Received: 27 March 2015 / Accepted: 9 June 2015 / Published online: 2 July 2015

Abstract We present theoretical results of a left-handed metamaterial engineered by a combination of coated and solid nano-spheres. The structure is a binary composite of CdS–TiO_2 core–shell and Au solid nano-spheres which simultaneously dispersed in the air matrix. The effective medium parameters derived by extended Maxwell-Garnett (*EMG*) effective medium theory. It is shown the possibility of fine-tuning the metamaterial in order to observe left-handed behavior. The results are supplemented with transmittance curves, calculated by layer-multiple-scattering (*LMS*) method. The predictions of the *EMG* theory are in good agreement with those of *LMS* method; thus the (CdS–TiO_2)/Au nano-composite is an appropriate choice as a three-dimensional left-handed metamaterial.

Keywords Metamaterial · Left-handed · Negative refraction index · Extended Maxwell-Garnett theory

1 Introduction

One important discovery has altered the electromagnetic radiation research over the last years. The concept of negative refraction index (*NRI*) has made greatly progress in the classical electrodynamics field. *NRI* can lead to a new class of devices (Veselago 1968; Smith et al. 2005; Pendry 2000) by offering unconventional properties which called left-handed behavior. Opposite phase and group velocities, negative refraction, absence of reflection, flat lens focusing and opposite radiation pressure is some of these amazing electromagnetic properties.

Both the permittivity and permeability must be negative simultaneously in order to achieve *NRI*. Natural materials with both ε and μ negative do not exist; hence the need for

✉ H. Sadeghi
H-Sadeghi@araku.ac.ir

[1] Department of Physics, Faculty of Science, Arak University, 8349-8-38156 Arak, Iran

artificial structures. Smith et al. built a structure with simultaneous negative ε and μ showing negative refraction for the first time (Shelby et al. 2001). The structure was a composite medium based on a periodic array of interspaced conducting nonmagnetic split ring resonators and continuous wires that exhibits a left-handed behavior in the microwave regime. There has been much progress in the development of *NRI* metamaterials which operate at microwave frequencies than for those at infrared and optical frequencies. However, there have been some recent attempts to propose structures of much simpler geometry than the common *NRI* metamaterials (split ring resonators and wires) which exhibit a frequency band with left-handed behavior at infrared frequencies. For instance, a *NRI* composite was reported which used two interpenetrating lattices of spheres (Yannopapas and Moroz 2005): one lattice used a polaritonic material to provide a negative permeability, and the other lattice used a Drude material to provide a negative permittivity. In constructing such structures the key concept is resonance. Indeed, near a resonance the response of a system to an electric field (as measured by the permittivity, ε) or to a magnetic field (as measured by the permeability, μ) exhibits a characteristic shape (Fig. 3). If the resonance is strong enough and sharp enough, there will be a frequency region where $Re(\varepsilon)$ or $Re(\mu)$ (or both) would be negative and $Im(\varepsilon)$ or $Im(\mu)$ would be very small. Recently, Foteinopoulou (2012) also demonstrated that polaritonic photonic crystal composites which consist of dielectric and polar material constituents arranged periodically in two dimensions (2D) can exhibit metamaterial parameters including magnetic behavior (negative permeability) at *THz* and mid-*IR* frequencies.

In this paper, we report on the design of a *NRI* metamaterial in the form of a binary composite which consists of both coated and solid nano-spheres in the air matrix. The respective binary composite is a 3D array of CdS–TiO_2 core–shell nano-spheres and *Au* solid nano-spheres which simultaneously embedded in the air matrix. To study this nano-composite theoretically, the extended Maxwell-Garnett (*EMG*) effective medium theory is used. Left-handed behavior is observed within a small frequency region. The results of the effective medium theory are supplemented with transmittance curves of light incident on a finite slab of a photonic crystal [the crystal consists of alternating planes of *Au* and (CdS–TiO_2) nano-spheres], calculated by layer-multiple-scattering (*LMS*) method.

The outline of the paper is as follows: Sect. 2 illustrates the effective-medium theory and show how the effective parameters for a composite arise within the context of an extended Maxwell-Garnett theory (*EMG*). Section 3 describes the structural properties of the (CdS–TiO_2)/*Au* composite. In the Sect. 4, the effective parameters of the simulated composite are presented and discussed. Finally, the main conclusions are summarized in Sect. 5.

2 Theory

A material composed of a mixture of distinct homogeneous media can be considered as a homogeneous one at a sufficiently large observation scale. The optical properties of such materials can be described in terms of effective medium theories. Effective medium theories define an effective index of refraction for a composite material in terms of the refractive indices of its components and their geometrical arrangement (Shalaev 2000). The most frequently used and most successful theories are Maxwell-Garnett (1904) (*MG*), Bruggeman (1935) (*BG*) and Lorentz-Lorenz (1880) (*LL*). The first two assume that the mixing materials are in separated phases. Typical dimensions of the constituent particles are supposed to be much smaller than the wavelength of the interacting radiation, but at the same time large enough to present their own electromagnetic behavior. *MG* considers the mixture that has separated a two-material grain structure where particles of the first material are dispersed in the continuous host of the second material. On the other hand, *BG* assumes an aggregate structure being a space-filling random mixture of two material phases. *LL* model is based on the Clausius–Mossotti equation and takes an average of molecular polarisability of the components. In this case no phase separation is considered. Depending on the level at which materials are mixed, one effective medium theory will be more appropriate than the other and will give more accurate prediction of the optical properties of the mixture. In this paper, the Maxwell-Garnett (*MG*) model for mixtures of spherical inclusions in a host continuum is explored.

We consider the case of small spherical particles having a complex dielectric constant ε_i, which are embedded, at a filling fraction f, in a host medium having a real dielectric constant ε_h. The effective dielectric constant ε_{eff} of a suspension of small spherical particles embedded in a host medium of dielectric constant ε_h is given by the Clausius–Mossotti equation

$$\frac{\varepsilon_{eff} - \varepsilon_h}{\varepsilon_{eff} + 2\varepsilon_h} = f\,\frac{\varepsilon_i - \varepsilon_h}{\varepsilon_i + 2\varepsilon_h} \tag{1}$$

Therefore, the *MG* effective dielectric function can be obtained through the relation

$$\varepsilon_{eff} = \varepsilon_h \frac{\varepsilon_i(1+2f) + 2\varepsilon_h(1-f)}{\varepsilon_i(1-f) + \varepsilon_h(2+f)} \tag{2}$$

The *MG* model includes interactions between the particles only through the Lorentz field, which limits its use to only small filling factors (Granqvist and Hunderi 1978). It usually describes an isotropic matrix containing spherical inclusions that are isolated from each other, such as the metal particles dispersed in a surrounding host matrix.

Heterogeneous materials (mixtures) that consist of too small particles compared to the wavelength of light are sub-wavelength structures (quasi-static approximation) which can only have effective electric responses (Aspnes 1982). An effective magnetic behavior will also arise if the constituent particles are sufficiently small to behave as a homogeneous material but still large enough for the Mie resonances to get excited. The quasi-static extension of the Maxwell-Garnett formula, also known as extended Maxwell-Garnett formula, can be obtained by Mie theory (Doyle 1989; Ruppin 2000). An incident plane wave, represented by the magnetic field $H_{inc} = H_0\, exp(ik_0 z)\, \hat{y}$ and $k_0 = w/c$, is incident on a single isolated sphere of radius r_0 and relative permittivity $\varepsilon_i = n^2$. The scattered magnetic field can be decomposed into multipole terms; the proportionality constant of the 2^m-pole term is

$$b_m = \frac{\psi_m(nx)\psi'_m(x) - n\psi_m(x)\psi'_m(nx)}{\psi_m(nx)\xi'_m(x) - n\xi_m(x)\psi'_m(nx)} \tag{3}$$

and the 2^m-pole coefficients of the scattered electric field are

$$a_m = \frac{n\psi_m(nx)\psi'_m(x) - \psi_m(x)\psi'_m(nx)}{n\psi_m(nx)\xi'_m(x) - \xi_m(x)\psi'_m(nx)} \tag{4}$$

Here $x = k_0 r_0$, and ψ_n and ξ_n are the Riccati–Bessel functions, and the primes indicate differentiation with respect to the argument. b_m and a_m are also known as Mie coefficients.

$m = 1$ corresponds to the dipole oscillation while $m = 2$ is associated with the quadrupole oscillation and so on. Only the b_1 coefficient, which is the strength of the magnetic dipole response, will be of interest when considering the effective permeability; only the a_1 term will be needed to find the effective permittivity. This yields the following extended *MG* formula

$$\varepsilon_{eff} = \frac{k_0^3 + 4i\pi N a_1}{k_0^3 - 2i\pi N a_1} \quad (5)$$

where N is the volume density of the dipoles. The filling fraction f of the composite is $f = 4\pi N r_0^3/3$, and should be kept to modest values. The optical properties of a suspension of small spheres may depend not only on the effective dielectric constant ε_{eff}, but also on the effective relative magnetic permeability μ_{eff}. The latter quantity can be different from unity, even when the inclusion and host materials are non-magnetic. This happens when the Mie coefficient b_1 which represents the magnetic dipole term is not negligible (Bohren 1986). In analogy with the derivation of (5), the effective permeability can be shown to be given by

$$\mu_{eff} = \frac{k_0^3 + 4i\pi N b_1}{k_0^3 - 2i\pi N b_1} \quad (6)$$

The effective index of refraction $n_{eff} = \sqrt{\varepsilon_{eff}\mu_{eff}}$ can be substituted in the Snell law to calculate the refraction of incident waves.

Now we consider the scattering by a homogeneous sphere coated with a homogeneous layer of uniform thickness (Bohren and Huffman 1983). Suppose that the electromagnetic wave is incident on a coated sphere with inner radius r_C and outer radius r_S (Fig. 1). The appropriate Mie coefficients are (n_C and n_S are the refractive indices of the core and coating),

Fig. 1 Modeling of a coated sphere

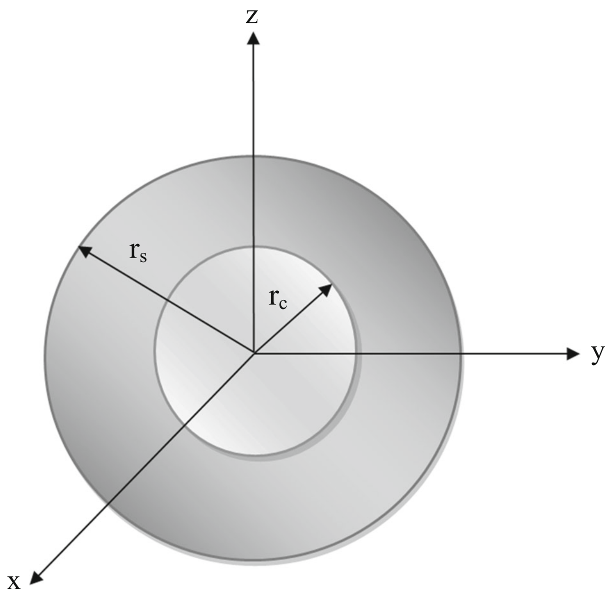

$$b_m = \frac{n_S\psi_m(y)[\psi'_m(n_Sy) - B_m\chi'_m(n_Sy)] - \psi'_m(y)[\psi_m(n_Sy) - B_m\chi_m(n_Sy)]}{n_S\xi_m(y)[\psi'_m(n_Sy) - B_m\chi'_m(n_Sy)] - \xi'_m(y)[\psi_m(n_Sy) - B_m\chi_m(n_Sy)]} \quad (7)$$

$$B_m = \frac{n_S\psi_m(n_Cx)\psi'_m(n_Sx) - n_C\psi_m(n_Sx)\psi'_m(n_Cx)}{n_S\chi'_m(n_Sx)\psi_m(n_Cx) - n_C\psi'_m(n_Cx)\chi_m(n_Sx)} \quad (8)$$

$$a_m = \frac{\psi_m(y)[\psi'_m(n_Sy) - A_m\chi'_m(n_Sy)] - n_S\psi'_m(y)[\psi_m(n_Sy) - A_m\chi_m(n_Sy)]}{\xi_m(y)[\psi'_m(n_Sy) - A_m\chi'_m(n_Sy)] - n_S\xi'_m(y)[\psi_m(n_Sy) - A_m\chi_m(n_Sy)]} \quad (9)$$

$$A_m = \frac{n_S\psi_m(n_Sx)\psi'_m(n_Cx) - n_C\psi'_m(n_Sx)\psi_m(n_Cx)}{n_S\chi_m(n_Sx)\psi'_m(n_Cx) - n_C\chi'_m(n_Sx)\psi_m(n_Cx)} \quad (10)$$

where $x = k_0r_C$, $y = k_0r_S$, $\chi_m(z) = -zy_m(z)$ and $y_m(z)$ is the spherical Bessel function of the second kind. To find the effective media values for coated spheres, we simply substitute these equations in Eqs. (5) and (6).

The effective permittivity, ε_{eff}, of a composite comprising two different kinds of solid spheres embedded in a matrix (binary composite) is given by

$$\sum_{j=A,B} C_j \frac{\varepsilon_h - \varepsilon_{eff} - \frac{3i}{2x_j^3}a_{1,j}f_{AB}(2\varepsilon_h + \varepsilon_{eff})}{\varepsilon_h + 2\varepsilon_{eff} - \frac{3i}{x_j^3}a_{1,j}f_{AB}(\varepsilon_h - \varepsilon_{eff})} = 0 \quad (11)$$

and the permeability, μ_{eff} by

$$\sum_{j=A,B} C_j \frac{\mu_h - \mu_{eff} - \frac{3i}{2x_j^3}b_{1,j}f_{AB}(2\mu_h + \mu_{eff})}{\mu_h + 2\mu_{eff} - \frac{3i}{x_j^3}b_{1,j}f_{AB}(\mu_h - \mu_{eff})} = 0 \quad (12)$$

where f_{AB} is the total filling factor of the spheres and the respective C_A and $C_B = 1 - C_A$ are the concentrations for the spheres A and B. In deriving (11) and (12) it has been assumed that the respective random unit-cell volumes of spheres A and B are proportional to the A and B sphere radii. Equations (11) and (12) provide a generalization of the earlier expressions for the effective permittivity and permeability, (5) and (6), to the two-sphere composite (Luo 1997).

The above mentioned effective medium theory can be used to study all the optical properties of the multiphase composites. In our previous works (Sadeghi et al. 2014a, b; Zolanvar et al. 2014), we have studied the optical properties of binary composites that consist of two different types of solid nano-spheres, one made from a dielectric material and the other from a plasmonic material, which are embedded in a host medium. Their electromagnetic responses have been studied using the extended Maxwell-Garnett effective medium theory. Such composites can show responses to an electric (magnetic) field at infrared frequencies which absolute values can be adjusted by controlling the filling fraction and size parameters. The magnetic dipole response is usually weak. This can be driven into resonance, however, by using materials with a large permittivity, such as ferroelectrics. However, their extreme permittivity drops off before infrared frequencies. Instead, the polaritonic resonances of crystals (reststrahlen region) can serve this purpose in the infrared (Huang et al. 2004). The large dielectric permittivity of the spheres also aids in scaling the resonances into the long-wavelength limit. The dielectric function in such materials is provided by the Drude–Lorentz model (Ibach and Luth 2003)

$$\varepsilon(\omega) = \varepsilon_\infty \left(1 + \frac{\omega_L^2 - \omega_T^2}{\omega_T^2 - \omega^2 - i\omega\gamma}\right) \tag{13}$$

where ε_∞ is the asymptotic value of the dielectric permittivity at high frequencies, γ is the damping constant, and the respective ω_T and ω_L are the transverse and longitudinal optical phonon frequencies.

In this work we are particularly interested in designing negative refraction index (*NRI*) materials, which requires both a negative permeability and a negative permittivity. Metals and Drude-like materials, which follow the Drude model dispersion, can provide the required negative material permittivity. The Drude model is given by

$$\varepsilon(\omega) = 1 - \frac{\omega_P^2}{\omega^2 + i\gamma\omega} \tag{14}$$

where ω_p is the bulk plasma frequency and γ is the damping term. Metals are the most familiar candidate for the plasmonic materials because metals tend to have large plasma frequencies and high electrical conductivity; they have traditionally been the materials of choice for plasmonics.

3 Description of the metamaterial composite

A negative refraction index (*NRI*) requires both a negative permeability and permittivity at the same frequency. Unfortunately, both cannot be made negative in the same frequency range. Nevertheless, the same concepts can be applied to more complex structures. We solve this problem by now considering coated spheres. We are ready to confront with a case of binary composite materials consisting of both coated and solid nano-spheres. The respective binary composite is a 3D array of CdS–TiO_2 core–shell nano-spheres and Au solid nano-spheres which simultaneously embedded in the air matrix. The resulting structure can also be visualized as two interpenetrating simple cubic lattices of the respective CdS–TiO_2 core–shell and Au nano-spheres. Therefore, this binary composite comprises two different kinds of non-overlapping nano-spheres with lattice constant $a = 1$ μm. Figure 2 shows a schematic of the (CdS–TiO_2)/Au binary composite.

Fig. 2 A schematic of the (CdS–TiO_2)/Au binary composite

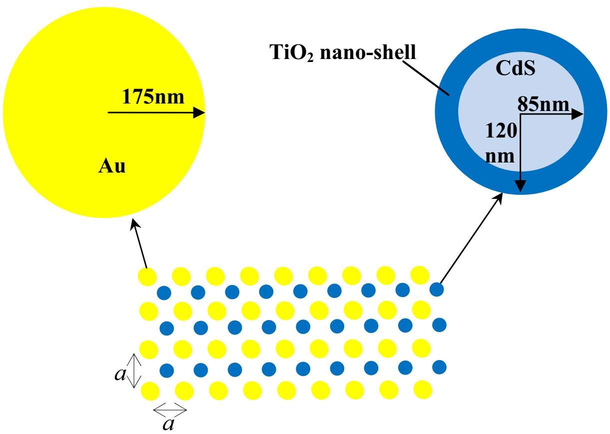

Technologically important semi conducting materials from II to VI group studied very intensively in the last two decades. Cadmium sulfide (*CdS*) is one of the cheapest semiconducting materials from same group. Already for some 100 years cadmium sulfide has been used as a pigment because of its color. It has a typical wide band gap of 2.4 eV at room temperature (Ashour 2003). The *CdS* compound semiconductors exhibit excellent electrical, chemical and optical properties which make them one of the promising candidates in the field of photovoltaic energy conversion. It provides useful properties for optoelectronic devices, such as photosensitive and photovoltaic devices or as photo-resistors. Also it is used in light amplifiers, radiation detectors, thin film transistor and diodes, piezoelectric transducers and laser. It thus is essential to explore the detailed optical and dielectric properties of *CdS* in the broad terahertz frequency region. So, the core material of the core–shell nano-spheres is assumed to be *CdS* with a radius of about 85 nm. For the shell material, we consider TiO_2 (anatase) with 35 nm thickness. The permittivity of both *CdS* and TiO_2 is described by Drude–Lorentz model (Eq. 13) which their parameters are characterized in Table 1. The damping constant for *CdS* and TiO_2 will be neglected for this study, i.e., we set $\gamma = 0$. The volume filling fraction occupied by *CdS*–TiO_2 nano-spheres is 0.368.

Previously mentioned that, in order to have *NRI*, what is required is a collection of nano-spheres with negative permittivity within all or part of the negative permeability region. For this purpose, *Au* solid nano-spheres whose permittivity is described by Eq. (14) with $\omega_p = 9.0$ (ev) and $\gamma = 0.072$ (ev) is chosen. The radius of the *Au* solid nano-spheres is 175 nm and the volume filling fraction occupied by this type of nano-spheres is 0.37. So, the total volume filling fraction occupied by the nano-spheres is about 0.74 (close-packed arrangement).

4 Results

In order to calculate the effective medium parameters of the (*CdS*–TiO_2)/*Au* nano-composite (described in previous section) within the context of the extended Maxwell-Garnett theory, we use and modify the code *EFFE2P* (http://www.wave-scattering.com/effe2p.f). Equations (11) and (12) are used in this code, with $C_A = C_B = 0.5$ for ε_{eff} and μ_{eff}, respectively. The resulting complex index of refraction is given by the branch of the square root ($n_{eff} = \sqrt{\varepsilon_{eff}\mu_{eff}}$) that yields a nonnegative imaginary part of n_{eff} along the positive real frequency axis.

The real and imaginary parts of ε_{eff}, μ_{eff} and n_{eff} for the (*CdS*–TiO_2)/*Au* nano-composite are shown in Fig. 3. It is evident that all the effective medium parameters exhibit strong resonant behavior which principally stems from the resonances of the electric (magnetic)-dipole components of the nano-spheres. *Au* nano-spheres are designed to have the electric-

Table 1 The parameters of the transverse (ω_T) and longitudinal (ω_L) optical phonon frequencies and the asymptotic value of the dielectric permittivity at high frequencies (ε_∞) for (*CdS*–TiO_2) nano-spheres

Material	($\omega_T/2\pi$) (THz)	($\omega_L/2\pi$) (THz)	ε_∞
CdS	7.01	9.14	15.13
TiO_2	10.97	22.54	5.41

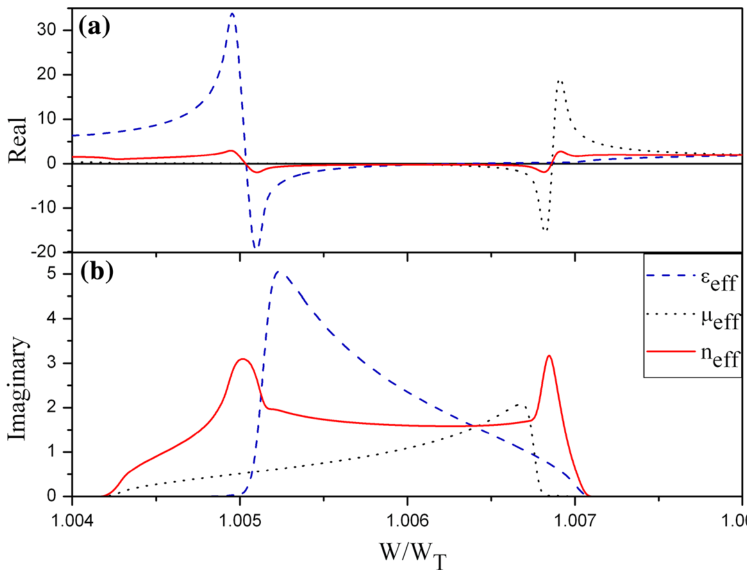

Fig. 3 **a** Real and **b** imaginary parts of ε_{eff}, μ_{eff} and n_{eff} for the (*CdS–TiO*$_2$)/*Au* nano-composite predicted by the extended Maxwell-Garnett theory. The radius of *Au* nano-spheres is 175 nm and the radius of (*CdS–TiO*$_2$) core–shell nano-spheres is 120 nm

dipole resonance while *TiO*$_2$ coating in (*CdS–TiO*$_2$) nano-spheres provides the magnetic one. However, the evanescent field within the coating can tunnel into the *CdS*.

In Fig. 3a one identifies a small area where all $Re\varepsilon_{eff}$, $Re\mu_{eff}$ and Ren_{eff} become negative within the same spectral region which is interpreted as left-handed behavior. Signs of real values of effective permittivity, permeability and index of refraction for the (*CdS–TiO*$_2$)/*Au* nano-composite, in terms of frequency changes, are given in Table 2. It is obvious that from $\omega/\omega_T = 1.0054$ to $\omega/\omega_T = 1.0063$ all the effective parameters assume negative values so the *NRI* metamaterial is evident. This is also shown the possibility of fine-tuning the light propagation in terms of frequency changes. By increasing the frequency, the right-handed behavior turns into the left-handed (from $\omega/\omega_T = 1.0054$ to $\omega/\omega_T = 1.0063$) and after this range it again changes to right-handed.

Within the *NRI* frequency region (Fig. 3b), the imaginary parts of ε_{eff}, μ_{eff} and n_{eff} are also significant. The imaginary part of the effective index of refraction is proportional to

Table 2 Sign of the real value of effective permittivity, effective permeability and effective index of refraction in terms of frequency changes for (*CdS–TiO*$_2$)/*Au* nano-composite

Composite	(1.004–1.005)	(1.005–1.0054)	(1.0054–1.0063)	(1.0063–1.0069)	(1.0069–1.008)
(*CdS–TiO*$_2$)/*Au*	$Re(\varepsilon_{eff}) > 0$	$Re(\varepsilon_{eff}) < 0$	$Re(\varepsilon_{eff}) < 0$	$Re(\varepsilon_{eff}) > 0$	$Re(\varepsilon_{eff}) > 0$
	$Re(\mu_{eff}) > 0$	$Re(\mu_{eff}) > 0$	$Re(\mu_{eff}) < 0$	$Re(\mu_{eff}) < 0$	$Re(\mu_{eff}) > 0$
	$Re(n_{eff}) > 0$	$Re(n_{eff}) < 0$	$Re(n_{eff}) < 0$	$Re(n_{eff}) < 0$	$Re(n_{eff}) > 0$

The radius of *Au* solid nano-spheres is 175 nm and the radius of (*CdS–TiO*$_2$) core–shell nano-spheres is 120 nm attenuation and has small values in this range. The presence of loss is an inevitable consequence of the underlying resonances, but the losses are smaller at frequencies away from the center of the lines.

In the (*CdS–TiO*$_2$)/*Au* metamaterial, the *NRI* region central frequency of $\omega = 1.0058\ \omega_T$ corresponds to the wavelength of $\lambda \approx 27.17$ μm. Therefore, the resulting structure is a sub-wavelength structure because the wavelength of light in the *NRI* region is almost 27 times larger than the lattice constant ($a = 1$ μm). This sub-wavelength structure with quasi-static approximation can provide both electric and magnetic responses.

It is worth noting that the left-handed behavior in this nano-composite depends on the fact that *Au* nano-spheres support localized surface plasmon resonances (*LSPRs*), which are excited when incident electromagnetic radiation creates coherent oscillations of the conduction electrons. *LSPRs* are also responsible for the enhancement of the electromagnetic fields surrounding *Au* nano-spheres. This unique property can be controlled through the main parameters of *Au* nano-spheres. The size of *Au* nano-spheres, for example, can have a significant effect on the optical properties of the nano-composite. In order to demonstrate the size effect we reduce the radius of *Au* nano-spheres to 165 nm while the radius of *CdS–TiO*$_2$ core–shell nano-spheres remains unchanged (120 nm). The real and imaginary parts of effective parameters for this nano-composite are shown in Fig. 4. The results are really interesting, even a small decrease in the size of *Au* nano-spheres can dramatically change the optical response of the (*CdS–TiO*$_2$)/*Au* nano-composite. For this nano-composite, contrary to the previous case, the left-handed behavior is not observed. In order to have more details, the signs of real values of effective parameters in terms of frequency changes are shown in Table 3. The effective index of refraction over the entire frequency range has positive values indicating that this nano-composite can't be a metamaterial. We have repeated the same process for different radius of *Au* nano-spheres.

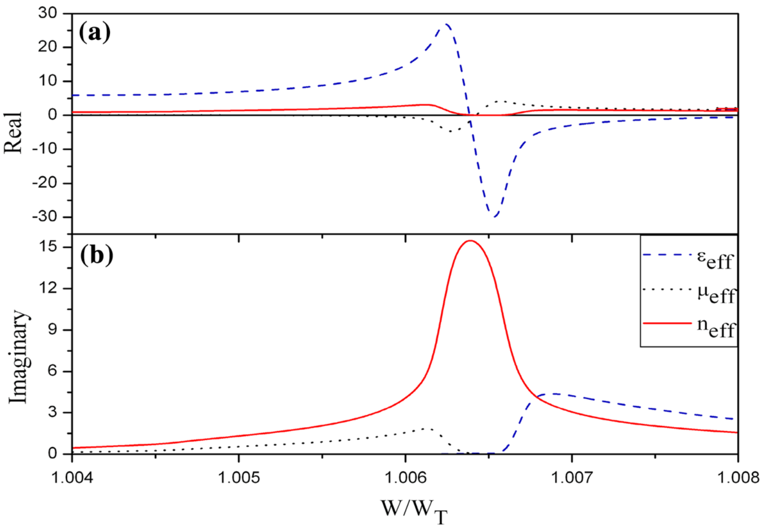

Fig. 4 **a** Real and **b** imaginary parts of ε_{eff}, μ_{eff} and n_{eff} for the (*CdS–TiO*$_2$)/*Au* nano-composite predicted by the extended Maxwell-Garnett theory. The radius of *Au* nano-spheres is 165 nm and the radius of (*CdS–TiO*$_2$) core–shell nano-spheres is 120 nm

Table 3 Sign of the real value of effective permittivity, effective permeability and effective index of refraction in terms of frequency changes for (CdS–TiO_2)/Au nano-composite

Composite	(1.004–1.0053)	(1.0053–1.0065)	(1.0065–1.008)
(CdS–TiO_2)/Au	$Re(\varepsilon_{eff}) > 0$	$Re(\varepsilon_{eff}) > 0$	$Re(\varepsilon_{eff}) < 0$
	$Re(\mu_{eff}) > 0$	$Re(\mu_{eff}) < 0$	$Re(\mu_{eff}) > 0$
	$Re(n_{eff}) > 0$	$Re(n_{eff}) > 0$	$Re(n_{eff}) > 0$

The radius of Au solid nano-spheres is 165 nm and the radius of (CdS–TiO_2) core–shell nano-spheres is 120 nm

The results show that the radius of Au nano-spheres in the (CdS–TiO_2)/Au nano-composite must be at least 175 nm in order to observe the *NRI* metamaterial.

We employ layer-multiple-scattering (*LMS*) method (Stefanou et al. 2000) which calculates the transmittance of light incident normally on a slab of a photonic crystal. The crystal consists of alternating planes of Au and (CdS–TiO_2) nano-spheres which has a periodic structure. The nano-spheres on each plane occupy the sites of a square lattice and the planes are arranged in which a succession of planes parallel to the (001) surface of *fcc* is formed. The *fcc* lattice can satisfy a close-packed arrangement of nano-spheres, so we choose this type of lattice. The lattice constant is $a = 1$ µm, and the Au nano-spheres have

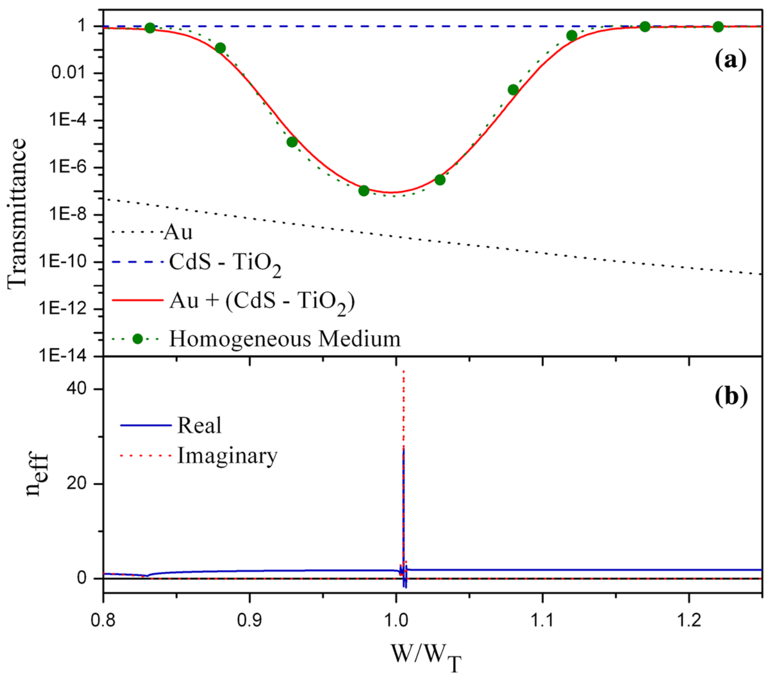

Fig. 5 **a** Transmittance curves (in log scale) for light incident normally on a slab of the crystal consisting of Au and (CdS–TiO_2) nano-spheres as calculated by the layer-multiple-scattering method. The slab consists of six layers (one layer contains two planes of spheres, one from each kind). **b** The real (*solid line*) and imaginary (*dotted line*) parts of n_{eff} for the (CdS–TiO_2)/Au nano-composite predicted by the extended Maxwell-Garnett theory

a radius of $0.175a$ while for the ($CdS–TiO_2$) nano-spheres the radius is $0.120a$. Figure 5a shows the transmittance of light incident normally [normal to the (001) surface] on a slab of the above crystal as obtained by the *LMS* method. The slab consists of six layers (one layer contains two planes of spheres, one from each kind). The transmission calculation is done for a transverse (*S*: the electric field parallel to the surface of the slab) incident wave. We identify a main gap where a dramatic reduction of the transmittance is occurred. In order to comparison, we also show the corresponding transmittance curves for the *fcc* planes that consist of only *Au* or ($CdS–TiO_2$) nano-spheres. We attribute the high transmittance of ($CdS–TiO_2$) nano-spheres to the fact that *CdS* and TiO_2 are both transparent materials. The effective medium theory results can be verified with the *LMS* method. To this end, we calculate the transmission of light on a slab of ($CdS–TiO_2$)/*Au* homogeneous medium which its effective parameters are calculated by the extended Maxwell-Garnett theory (ε_{eff} and μ_{eff}). The curves verify our design and also the effective medium theory.

In Fig. 5b we show the real (solid line) and imaginary (dotted line) parts of effective index of refraction n_{eff} for the ($CdS–TiO_2$)/*Au* nano-composite as obtained from the extended Maxwell-Garnett theory. We observe that the region where the real part of n_{eff} is negative correlates very well with the gap of the transmittance curve. This is due to losses in *Au* nano-spheres that stem from large imaginary part of gold permittivity which basically specifies the sign of effective index of refraction (Fig. 3). An important point to notice is that the extended Maxwell-Garnett prediction of negative n_{eff} is in good agreement with that of the *LMS* method.

5 Conclusions

In this work we have shown how a left-handed metamaterial can be achieved by a composite that composed of coated and solid nano-spheres. The respective composite is a 3D array of $CdS–TiO_2$ core–shell and *Au* solid nano-spheres. We have used Mie scattering theory in an effective medium approach which accurately predicts the effective medium parameters of the composite. Our results provide the possibility of fine-tuning the metamaterial in terms of frequency changes. In order to show the size effect we have reduced the radius of *Au* nano-spheres. Interestingly, the left-handed behavior completely disappears in the whole frequency range. The results for the effective index of refraction have been supplemented by layer-multiple-scattering (*LMS*) calculations of light-transmittance curves from a finite slab of alternating planes of *Au* and ($CdS–TiO_2$) nano-spheres. The overall findings provide useful information for the design of practical devices with left-handed behavior in *THz* region.

References

Ashour, A.: Physical properties of spray pyrolysed CdS thin films. Turk. J. Phys. **27**, 551–558 (2003)

Aspnes, D.E.: Local-field effects and effective-medium theory: a microscopic perspective. Am. J. Phys. **50**, 704–709 (1982)

Bohren, C.: Applicability of effective-medium theories to problems of scattering and absorption by nonhomogeneous atmospheric particles. J. Atmos. Sci. **43**, 468–475 (1986)

Bohren, C.F., Huffman, D.R.: Absorption and Scattering of Light by Small Particles. Wiley-Interscience, New York (1983)

Bruggeman, D.A.: Calculation of various physics constants in heterogenous substances I. Dielectricity constants and conductivity of mixed bodies from isotropic substances. Ann. Phys. **24**, 636–664 (1935)

Doyle, W.T.: Optical properties of a suspension of metal spheres. Phys. Rev. B **39**, 9852–9858 (1989)

Foteinopoulou, S.: Photonic crystals as metamaterials. Phys. B **407**, 4056–4061 (2012)

Granqvist, C.G., Hunderi, O.: Optical properties of Af–SiO_2 cermet films: a comparison of effective medium theories. Phys. Rev. B **18**, 2897–2906 (1978)

Huang, K.C., Povinelli, M.L., Joannopoulos, J.D.: Negative effective permeability in polaritonic photonic crystals. Appl. Phys. Lett. **85**, 543–545 (2004)

Ibach, H., Luth, H.: Solid-State Physics. Springer, Berlin (2003)

Lorenz, L.: Ueber die Refractionsconstante. Ann. Phys. **11**, 70–103 (1880)

Luo, R.: Effective medium theories for the optical properties of three-component composite materials. Appl. Opt. **36**, 8153–8158 (1997)

Maxwell-Garnett, J.C.: Colours in metal glasses and in metallic films. Philos. Trans. R. Soc. Lond. Ser. A **203**, 385–420 (1904)

Pendry, J.B.: Negative refraction makes a perfect lens. Phys. Rev. Lett. **85**, 3966–3969 (2000)

Ruppin, R.: Evaluation of extended Maxwell-Garnett theories. Opt. Commun. **182**, 273–279 (2000)

Sadeghi, H., Zolanvar, A., Ranjgar, A., Norouzi, R.: Terahertz response of ZnS/Ge and ZnO/Ge nanostructured composites. Plasmonics **9**, 327–333 (2014a)

Sadeghi, H., Zolanvar, A., Ranjgar, A., Norouzi, R.: Effective permittivity and refractive index of TiO_2/Ge and SiO_2/Ge nanostructures at high frequencies. J. Electron. Mater. **43**(11), 4294–4300 (2014b)

Shalaev, V.M.: Nonlinear Optics of Random Media: Fractal Composites and Metal-Dielectric Films. Springer, Berlin (2000)

Shelby, R.A., Smith, D.R., Schultz, S.: Experimental verification of a negative index of refraction. Science **292**, 77–79 (2001)

Smith, D.R., Pendry, J.B., Wiltshire, M.C.K.: Metamaterials and negative refractive index. Science **305**, 788–792 (2005)

Stefanou, N., Yannopapas, V., Modinos, A.: MULTEM 2: a new version of the program for transmission and band-structure calculations of photonic crystals. Comput. Phys. Commun. **132**, 189–196 (2000)

The code EFFE2P can be downloaded from http://www.wave-scattering.com/effe2p.f

Veselago, V.G.: The electrodynamics of substances with simultaneously negative values of ε and μ. Sov. Phys. Usp. **10**(4), 509–514 (1968)

Yannopapas, V., Moroz, A.: Negative refractive index metamaterials from inherently non-magnetic materials for deep infrared to terahertz frequency ranges. J. Phys. Condens. Matter **17**, 3717–3734 (2005)

Zolanvar, A., Sadeghi, H., Ranjgar, A.: Effective dielectric properties of Au–ZnS and Au–ZnO plasmonics nanocomposites in the terahertz regime. Chin. Phys. Lett. **31**(10), 106201 (2014)